

Coarctate and Möbius: The Helical Orbitals of Allene and Other Cumulenes

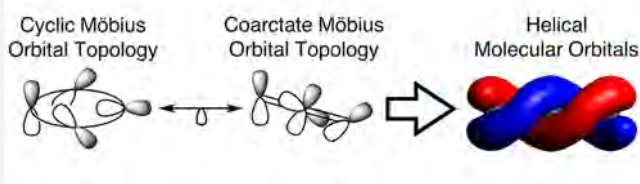
Marc H. Garner,^{*,†,‡,§} Roald Hoffmann,^{*,§} Sten Rettrup,[†] and Gemma C. Solomon^{†,‡}

[†]Department of Chemistry and [‡]Nano-Science Center, University of Copenhagen, Universitetsparken 5, DK-2100, Copenhagen Ø, Denmark

[§]Department of Chemistry and Chemical Biology, Cornell University, Ithaca, New York 4850, United States

S Supporting Information

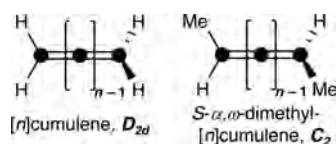
ABSTRACT: As brought to the attention of the community by Hendon et al. and noted by previous workers, the π orbitals of the equilibrium geometry odd-carbon (even number of double bonds = n) $[n]$ cumulenes may be written in either rectilinear or helical form. We trace the origins and detailed composition of the helical orbitals of cumulenes, which emerge in the simplest Hückel model and are not much modified in advanced computations. For the α,ω -disubstituted even $[n]$ cumulenes, the helical representation is obligatory as the symmetry is reduced from D_{2d} to C_2 . A relationship is apparent between these helical orbitals of the even $[n]$ cumulenes, seen as a Herges coarctate system, and the corresponding Möbius cyclic polyene orbitals. The twist of the orbitals varies in interesting ways along the helix, and so does the contribution of the component atomic orbitals. Though the electronic structures of even $[n]$ cumulenes and Möbius cyclopolyenes are closely related, they differ for higher n in intriguing ways; these are linked to the constrained rotation of the basis orbitals along the helical twist itinerary. Relations are constructed between the level patterns of the π -systems of even $[n]$ cumulenes and ideas of Hückel and Möbius aromaticity.



INTRODUCTION

Cumulenes (Scheme 1) are a class of linearly conjugated π -systems akin to alkynes, but terminated by tricoordinate carbon

Scheme 1. $[n]$ Cumulenes



atoms. By convention, we label the molecules by n , the number of cumulated double bonds; the number of carbon atoms is then $n + 1$. For $[n]$ cumulenes with even n , the terminal carbon atoms are mutually perpendicular in order to form closed-shell π -systems. We will denote these molecules from here on as “even” $[n]$ cumulenes.

In unsubstituted even $[n]$ cumulenes, the frontier π molecular orbitals (MOs) are all explicitly degenerate, a consequence of the ideal D_{2d} symmetry of the molecule. The degeneracy of the orbitals is lifted by α,ω -disubstitution, which reduces the symmetry of the molecule to C_2 or lower, making it chiral. The degeneracy may also be broken by axial torsion toward the achiral planar transition state for mutual rotation of the end carbons, for example, through mechanical strain.^{1–7} A consequence of the perpendicular end-groups is that these molecules may be considered to have helical frontier orbitals, as recently explored by Hendon et al.,⁸ an effect they coined “electrohelicality”. This

helicity is also the primary concern of our work, and we will elaborate the concept in some detail.

Perhaps it is best to introduce the subject pictorially. In Figure 1 we show from a density functional theory (DFT) calculation (details below) the four occupied π MOs of $[4]$ cumulene (left) and of S -1,5-dimethyl- $[4]$ cumulene (right). The specific choice of MOs made for $[4]$ cumulene itself is to a degree arbitrary, as we will see. That for the 1,5-dimethyl compound is not. We have here a chemically minor perturbation, yet the orbitals have a very different appearance. But how different are they? And from where the distinctive helicity of the orbitals of the dimethyl derivative? These are the questions we will explore, as well as a fascinating topological connection of the even $[n]$ cumulenes to Möbius conjugation.

Allene and Higher Cumulenes. The shortest even $[n]$ cumulene, allene, is a common starting material in organic syntheses; the variety of synthesized derivatives is immense.^{9–18} Successful syntheses of the longer even $[n]$ cumulenes are sparse, most likely due to their high reactivity. Still a number of $[4]$ cumulenes^{19–29} and a few metallo- $[6]$ cumulenes^{30–32} have been reported. In comparison, odd $[n]$ cumulenes have been synthesized and characterized up to $[9]$ cumulene,^{33–35} while polyynes have been made with up to 44 carbon atoms.^{36–38} Ingenious strategies are being developed to further stabilize these otherwise highly reactive molecules, including protection with a

Received: February 5, 2018

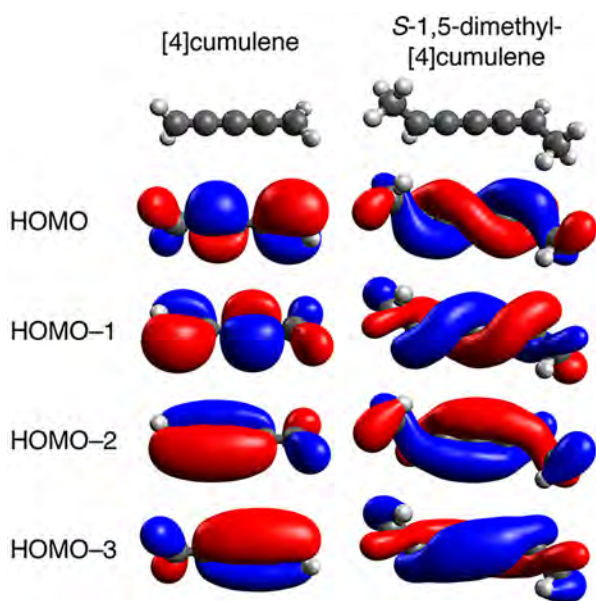


Figure 1. Optimized structure and bonding π molecular orbitals of [4]cumulene (pentatetraene) and S-1,5-dimethyl-[4]cumulene.

rotaxane ring,³⁹ and growth of carbon wires inside carbon nanotubes;⁴⁰ similar strategies may hold great promise for stabilizing even $[n]$ cumulenes.

The α,ω -disubstituted, chiral $[n]$ cumulenes attracted much attention in early synthetic work, and a number of allenes and [4]cumulenes were successfully synthesized and characterized, including the aforementioned α,ω -dimethyl substituted species, which have C_2 symmetry, studied by Hendon et al.⁸ (Scheme 1, right).^{21,22,41–44} Early studies had a particular focus on the chiroptical properties of allene. Though the researchers active in the field probably did not realize at the time that some of the allenes have helical orbitals, they certainly were aware that the chirality and reduced symmetry of the molecules had implications for their electronic structure. We quote from Richardson and co-workers (1976)² on the vertical excitation in axially twisted allene: “The helicity of each of these structures is M (left-handed screw sense about the C=C=C bond axis), and in a classical sense the chromophoric π -electrons may be pictured as following a helical trajectory along (and about) the C=C=C bond axis when involved in $\pi \rightarrow \pi^*$ transitions in these structures.”

Cumulene synthesis has seen renewed attention in recent years, particularly due to the broad interest in making and studying *karbin* or carbyne, the infinite chain carbon allotrope.^{38,45} From the perspective of carbyne, the perpendicular end-groups of even $[n]$ cumulenes are an edge-effect of the material.

The Möbius Topology and Cumulenes. Shown in Figure 2, the basis p-orbitals on a Möbius strip have continuous if diminished overlap. The overlap may be decreased in size by further deformations caused by the underlying σ system in molecules. In the simplest Möbius topology, there is one change of sign in the final overlap of the basis set, as the band closes. Molecules with $4n$ electrons in such a π -system are a closed-shell system, and may be thought of as aromatic, in tentative analogy to $4n+2$ Hückel aromatic systems. The idea is due to Heilbronner;⁴⁶ we refer to the extensive work of Herges, Mauksch, Rzepa, and Schleyer for more detailed descriptions of Möbius aromaticity.^{47–54}

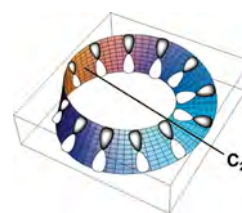


Figure 2. Möbius orbital topology. Basis set p-orbitals placed on the surface of a Möbius band results in one sign inversion in the overlaps. Reproduced from Rzepa, H. S. Möbius Aromaticity and Delocalization. *Chem. Rev.* **2005**, *105*, 3697–3715 (ref 51). Copyright 2005 American Chemical Society.

Due to the twist of the “band,” the highest achievable symmetry of a Möbius system is C_2 , as Figure 2 shows, or C_n if there are multiple twists of 180° (here n is the integer number of twists).^{47,48,51} Extensive work has been put into synthesizing Möbius aromatic molecules; the efforts resulted in the first such systems in 2003.^{55–57} The molecules made are large cyclic π systems, some retaining C_2 symmetry.^{55,58,59} It has been noted that allenic units incorporated in annulenes can also give rise to Möbius aromaticity, due to a sign change in the basis.^{60,61}

Following Heilbronner’s original conception of Möbius π -electron systems in 1964,⁴⁶ it was noted by Fischer and Kollmar in 1968,⁶² and independently by Zimmerman in 1971,⁶³ that the basis π orbitals of allene actually have a Möbius topology and the MOs behave accordingly. The topology of orbital interactions in allene may be seen in Figure 3 at right; below it is a “few frame”

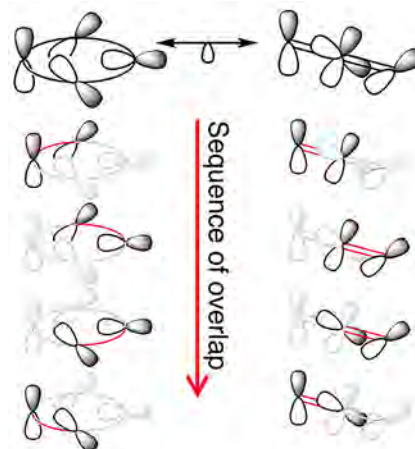


Figure 3. Möbius orbital topology of cyclic and linear systems. (Top) Basis orbitals of a four-site cyclic Möbius model and allene ([2]cumulene). (Bottom) Animated sequence of orbital overlaps around the Möbius basis, and “back-and-forth” for the allene basis. Note the sign change in the final interaction. In equivalence to cyclic Möbius topology, by topology allene is a coarctate Möbius system.

animation showing the sequence of orbital overlaps. To the left of this animation are the corresponding orbital overlaps in a fictitious Möbius cyclobutadiene. The analogy is obvious. And its consequences are a two below two π -orbital energy scheme for both Möbius cyclobutadiene, a most unrealistic system, and allene, very much a real molecule.

It also makes sense to call the allene orbital system a *coarctate* one. The word was coined by Herges in the context of his useful classification of those pericyclic reactions in which two participating π -systems are fused or merged.^{64–69} General for

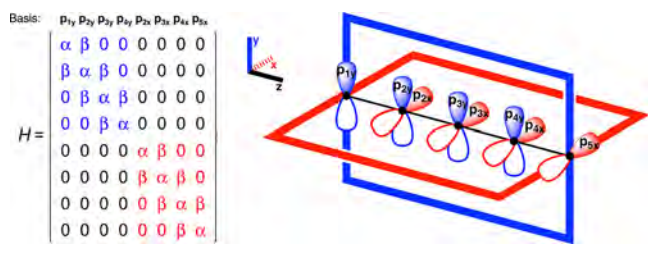
the π -system of even $[n]$ cumulenes is that, quite analogous to the case of allene, they can be described in a basis with one sign change in the basis set orbital overlap sequence, and thus they are all topologically coarctate Möbius systems. In this work, we reexamine the relation between the Möbius orbital topology and the helical MOs of even $[n]$ cumulenes, 50 years after the connection was originally noted by Fischer and Kollmar.⁶²

PERPENDICULAR AND HELICAL MOLECULAR ORBITALS

It is instructive to approach the helical and perpendicular representations of the π molecular orbitals of an even $[n]$ cumulene using a Hückel or tight-binding model that captures the essence of the orbitals. In the ensuing discussion we will focus on $[4]$ cumulene (pentatetraene) rather than the smallest member of the even n series, allene ($[2]$ cumulene). The reason for doing so is that some of the special features of orbital rotation, or twist, and of “size” emerge more clearly in the $[4]$ cumulene.

The standard basis set for $[4]$ cumulene consists of two perpendicular sets of p-orbitals labeled in Scheme 2. We set the

Scheme 2. Hückel Matrix and Orbital Basis for Pentatetraene



coulomb integral (on-site energy) $\alpha = 0$ and report the eigenvalues in energy units of β , the resonance integral (transfer integral) describing the in-phase nearest neighbor interactions. β is negative. The corresponding Hamiltonian (Scheme 2, left) is block-partitioned; i.e., there are no nonzero matrix elements between the first block of four ($2p_y$ orbitals, blue) and the second block of four ($2p_x$ orbitals, red).

Solving the eigenvalue problem of the Hückel Hamiltonian (Scheme 2, left) leads to MOs of two perpendicular π systems. The bonding MOs among these are shown in Figure 4 and listed in the left column of Table 1. The shapes of these MOs are trivial; they are those of the two idealized butadiene systems (there is no provision made here for bond alternation; it can be done,⁷⁰ but the alternation is small in both even and odd $[n]$ cumulenes³⁵), perpendicular to each other and displaced by one carbon atom (along the z -axis). Consequently, the π eigenfunctions come in degenerate pairs and belong to the ϵ irreducible representation of the D_{2d} point group. Antibonding orbitals are not shown; they are “paired” with the bonding orbitals in a way we know well for alternant hydrocarbons.⁷¹

The MOs shown in the left column of Figure 4 are appropriate to D_{2d} symmetry. But, of course, they are not unique. Given the

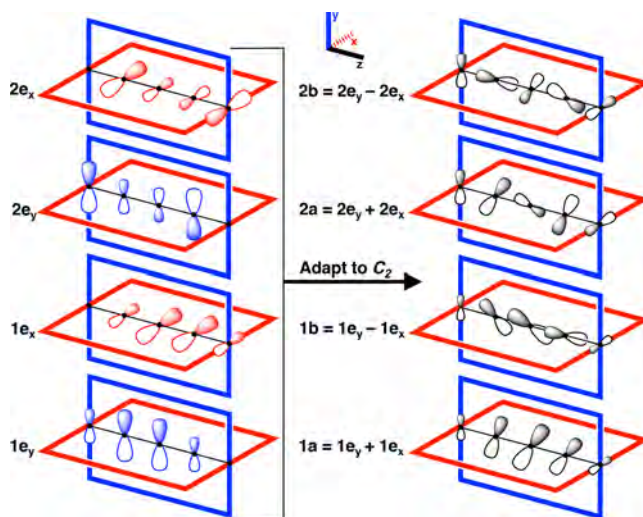


Figure 4. (Left column) “Perpendicular” bonding MOs of $[4]$ cumulene which are symmetry-adapted to D_{2d} , emphasizing the mirror planes in this point group. (Right column) Bonding MOs, now symmetry-adapted to C_2 ; these are the helical solutions. Each quasi-degenerate pair forms a right-handed and a left-handed helix.

Table 1. Bonding Hückel MOs for $[4]$ Cumulene from the Perpendicular Basis Set Shown in Figure 4^a

	Atom	LCAO (D_{2d})					LCAO (C_2)					MO
		1	2	3	4	5	1	2	3	4	5	
		p_{1y}	p_{2y}	p_{3y}	p_{4y}		p_{1y}	p_{2y}	p_{3y}	p_{4y}		
$\epsilon \cdot \beta^{-1}$	MO		p_{2x}	p_{3x}	p_{4x}	p_{5x}		p_{2x}	p_{3x}	p_{4x}	p_{5x}	MO
0.62	$2e_x$	+ 0.00	+ 0.00	+ 0.00	+ 0.00		+ 0.43	+ 0.26	- 0.26	- 0.43		2b
			+ 0.60	+ 0.37	- 0.37	- 0.60		- 0.43	- 0.26	+ 0.26	+ 0.43	
0.62	$2e_y$	+ 0.60	+ 0.37	- 0.37	- 0.60		+ 0.43	+ 0.26	- 0.26	- 0.43		2a
			+ 0.00	+ 0.00	+ 0.00	+ 0.00		+ 0.43	+ 0.26	- 0.26	- 0.43	
1.62	$1e_x$	+ 0.00	+ 0.00	+ 0.00	+ 0.00		+ 0.26	+ 0.43	+ 0.43	+ 0.26		1b
			+ 0.37	+ 0.60	+ 0.60	+ 0.37		- 0.26	- 0.43	- 0.43	- 0.26	
1.62	$1e_y$	+ 0.37	+ 0.60	+ 0.60	+ 0.37		+ 0.26	+ 0.43	+ 0.43	+ 0.26		1a
			+ 0.00	+ 0.00	+ 0.00	+ 0.00		+ 0.26	+ 0.43	+ 0.43	+ 0.26	

^aThe LCAO-MOs can be symmetry-adapted from D_{2d} to C_2 to form the helical solutions.

MO pairs are explicitly degenerate, any linearly independent combination of a pair of degenerate solutions will be an equally valid solution. The particular set of MOs chosen in the left columns of Figure 4 and Table 1 “emphasizes” the mirror planes of the D_{2d} structure, perhaps we can call it the “rectilinear” choice. Alternative combinations may be formed to emphasize the C_2 axes in D_{2d} ; these axes are shown in Figure 5.

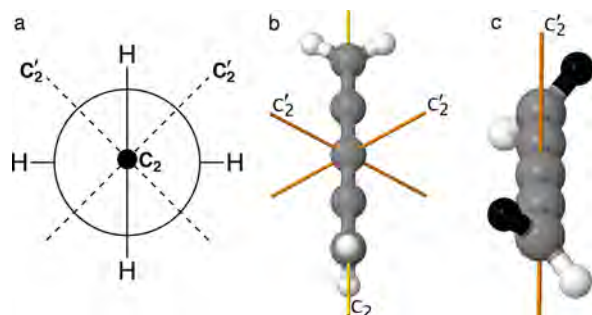


Figure 5. C_2 axes of [4]cumulene. Unsubstituted [4]cumulene has three C_2 axes, specified in a Newman projection along the carbon-axis (a), and in another view (b). Two of the C_2 axes are helicogenic (orange), and one is not (yellow). In 1,5-disubstituted-[4]cumulenes (c) only the one helicogenic C_2 axis (perpendicular to carbon axis) remains.

Following α,ω -disubstitution only one of these C_2 axes remains. This is the axis that carries the two substituents into each other, as shown in Figure 5 on the right. General for the series of even $[n]$ cumulenes, the MOs that emphasize the remaining C_2 axis become the *only* solutions appropriate to the reduction in symmetry from D_{2d} to C_2 upon α,ω -disubstitution. These are in fact the helical MOs shown in the right column of Figure 4; the same MOs were shown for the 1,5-disubstituted [4]cumulene in Figure 1, albeit from a DFT calculation. We will call this crucial C_2 axis helicogenic.

Derivation of the Helical Molecular Orbitals. What do the C_2 -adapted wave functions look like? One can either redo the process of forming symmetry-adapted linear combinations in C_2 symmetry, following the standard procedures of the theory of group representations, described in detail in textbooks, e.g., that of Cotton.⁷² Or one can use symmetry reduction correlation tables.⁷³ Either way, an E representation in D_{2d} becomes A + B in C_2 symmetry. The *a* and *b* combinations can be written as follows:

$$a = \frac{1}{\sqrt{2}}(e_y + e_x)$$

$$b = \frac{1}{\sqrt{2}}(e_y - e_x)$$

The resulting molecular orbitals are given for 1e and 2e at the right of Table 1, and are drawn at the right of Figure 4. These MOs are the only set that is symmetry-adapted to the C_2 symmetry of the 1,5-disubstituted-[4]cumulene. And these orbitals correspond precisely to the helical MOs we show in Figure 1; as a consequence of the reduction in symmetry, the MOs are no longer explicitly degenerate and may split, though not by much in the dimethyl case shown.⁸

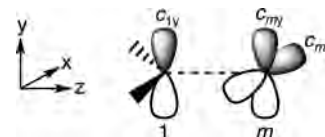
So far things are relatively simple—there are two equivalent representations of the [4]cumulene (or for that matter, all even $[n]$ cumulenes). One is “rectilinear” or D_{2d} -like. The other is helical. Now things become slightly more complicated.

Calculating the Twist of a Molecular Orbital: The Helix Is Imperfect. In making precise the helical character of a given Hückel MO, we need to calculate the relative twist angle of two atomic orbitals which enter an MO. The π orbitals emerge from a calculation in the following form:

$$\psi = c_{1x}p_{1x} + c_{1y}p_{1y} + \dots + c_{mx}p_{mx} + c_{my}p_{my}$$

where the basis orbitals are shown in Scheme 3.

Scheme 3. Basis Set and Axis Definition for a Cumulene



We utilize the fact that p-orbitals transform as vectors. The angle A between two arbitrary vectors, v and w , is given in eq 1.

$$A_{\vec{v}-\vec{w}} = \cos^{-1}\left(\frac{\vec{v} \cdot \vec{w}}{|\vec{v}| \cdot |\vec{w}|}\right) \quad (1)$$

Given the arbitrary absolute coordinate system shown in Scheme 3, $c_{1x} = 0$, as there is no p_x component on atom 1. The angle A_{1m} , between the p-orbital on atom 1 and the orbital on atom m that is described by $c_{mx}p_{mx} + c_{my}p_{my}$ is

$$\begin{aligned} A_{1m} &= \cos^{-1}\left(\frac{\begin{bmatrix} 0 \\ c_{1y} \end{bmatrix} \cdot \begin{bmatrix} c_{mx} \\ c_{my} \end{bmatrix}}{\sqrt{c_{1y}^2} \cdot \sqrt{c_{mx}^2 + c_{my}^2}}\right) \\ &= \cos^{-1}\left(\frac{c_{my}}{\sqrt{c_{mx}^2 + c_{my}^2}}\right) \end{aligned} \quad (2)$$

Using this procedure, we evaluate the degree of twist at each atom using the MO coefficients of Table 1 and eq 2. The outcome is summarized graphically in Figure 6.

It is clear that there is a direct connection between the writhe (we use the word colloquially here) of the MOs and their eigenvalues; the higher energy ones twist more, as expected. One reason we moved from allene ($n = 2$) to pentatetraene ($n = 4$) is that there are interesting aspects to the twist of the helical orbitals. Each pair of MOs ($1a + 1b, 2a + 2b$) consists of a *P* and an *M* helix. $1a + 1b$ twist by a total of $\pm 90^\circ$ from atom 1 to 5, and $2a + 2b$ by $\pm 270^\circ$. But each helical orbital (at atoms 2, 3, 4) is not required by symmetry to twist by $90^\circ/4 = 22.5^\circ$ or $270^\circ/4 = 67.5^\circ$ relative to its neighboring atoms.

The MOs do not have an even distribution of the helical twist. As Figure 6 shows graphically, in $1a$ and $1b$, the twist is, so to speak, more localized on the edges of the molecule. That is, the twist is “faster” from carbon 1 (purple) to carbon 2 (blue) at $\pm 32^\circ$, than for carbon 2 (blue) to carbon 3 (green) twisting by 13° (from $\pm 32^\circ$ to $\pm 45^\circ$). In $2a$ and $2b$ the “twist-localization” is reversed. There the twist is localized in the central part of the molecule; from atom 1 (purple) to atom 2 (blue) the twist is $\pm 58^\circ$, and from atom 2 (blue) to atom 3 (green) the twist is 77° (from $\pm 58^\circ$ to $\pm 135^\circ$).

In hypothetical Möbius systems of the “normal” non-cumulene type, the assumption usually is that the twist proceeds equally distributed along the cycle. But in the synthetically

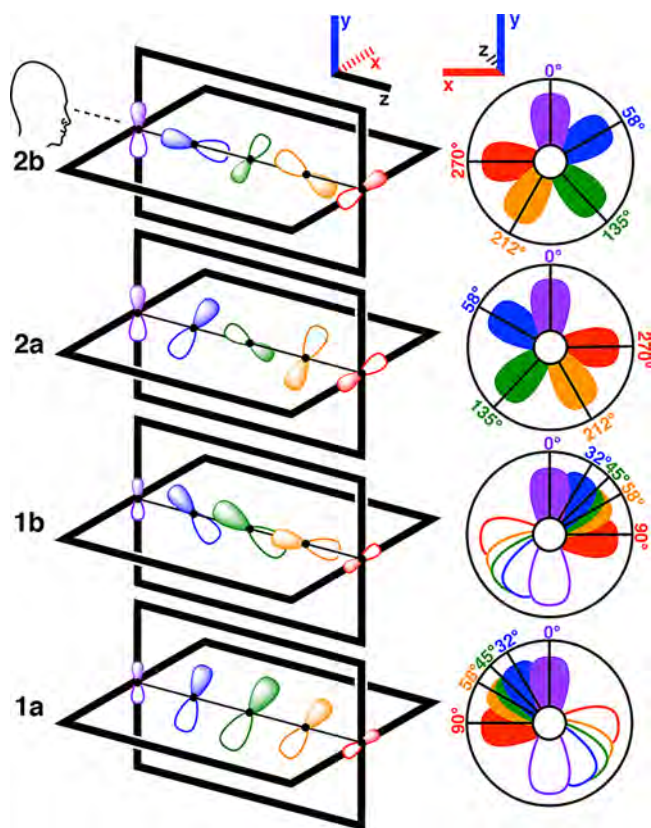


Figure 6. (Left) Helical MOs of [4]cumulene colored by atom site (from violet to red). (Right) Diagrammatic representation of the twist angles of the MOs projected along the z -axis. For 2a and 2b, only the positive lobes of the orbitals are plotted for clarity. The a orbitals form an imperfect M -helix, and the b orbitals form an imperfect P -helix.

realized cyclic Möbius annulenes and porphyrins, the twist also “localizes,” principally as a consequence of the constraints of the underlying σ -orbital system.^{58,74,75} In cumulenes, the twist-localization is a consequence of the π -system itself. There are consequences for the energetics; we will return to these.

Orbital “Sizes” Along the Helix. The reader will have noticed two related details in the helical C_2 representation of the 1e (1a + 1b) and 2e (2a + 2b) orbitals on the right of sides of Figure 4 and Table 1: the contributions of the p_y basis functions at atoms 1 and 4 are of equal weight to those of the p_x basis functions at atoms 2 and 5. However, as a consequence of the displacement of the p_x and p_y coefficients by one atom, their contributions at each atom are quite different from each other, except for atom 3. This can be expressed in another way: The x and y components of the orbitals making up the helix have unequal “size” along the carbon axis, growing “fat” or “slim” along it.

The size of the orbitals on each atom is related simply (in the underlying Hückel model) by the square root of sums of squares of the p_x and p_y contributions. The resulting MO coefficient, c , which has both an x and y component, is related to its two component coefficients by

$$c^2 = \frac{1}{2}(c_x^2 + c_y^2) \quad (3)$$

The MO coefficients grow from the end toward the middle in 1a + 1b, while the coefficients are smallest in the middle of the more tightly wound helix in 2a + 2b.

We have now seen that even in the Hückel model there are special features to the beautiful helical orbitals—in their detailed composition and in the varying degree of twist of the component atomic orbitals. What changes if we progress from a Hückel model to wave function based or DFT calculations?

BEYOND THE HÜCKEL MODEL

In the introduction we showed the actual π molecular orbitals as they emerge from a DFT calculation. Let us describe these in further detail. The calculations for [4]cumulene and *S*-1,5-dimethyl-[4]cumulene were carried out with DFT to the *verytight* criteria using the M06-2X⁷⁶ functional with 6-311G-(d,p) basis as implemented in Gaussian09.⁷⁷ The optimizations were performed with *ultrafine* grid for calculating integrals and loose symmetry constraint to D_{2d} point group symmetry for [4]cumulene, and C_2 for 1,5-dimethyl-[4]cumulene. The isosurfaces of the MOs are plotted in Figure 1 and 7 using the standard iso value of 0.02.

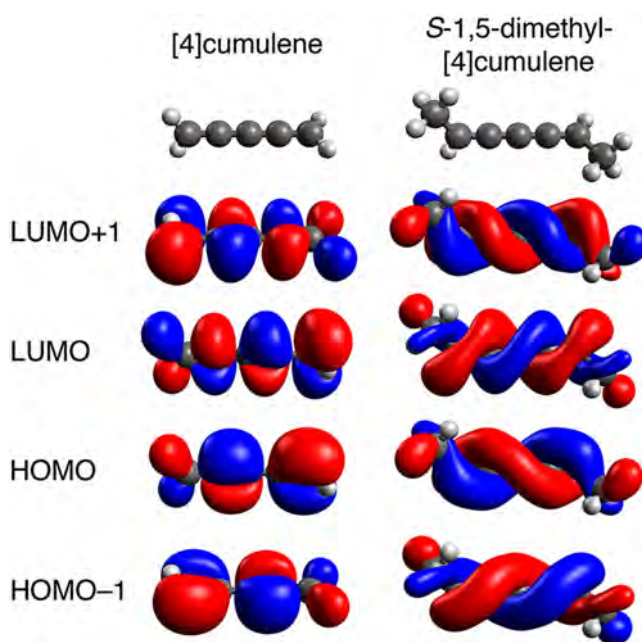


Figure 7. Optimized structure and frontier π molecular orbital pairs of [4]cumulene (pentatetraene) and *S*-1,5-dimethyl-[4]cumulene.

Not much changes. We have already noted the main features of these orbitals—the rectilinear or perpendicular choice of orbitals in the D_{2d} geometry in Figure 1, with the arbitrariness of that choice made clear in an earlier section. And we see the clearly helical nature of the orbitals in *S*-1,5-dimethyl-[4]cumulene. The orbitals come in degenerate or quasi-degenerate pairs, with increasing number of nodes with energy as anticipated; the LUMO and LUMO+1 of the same two molecules shown in Figure 7. There is substantial hyperconjugation to the terminal CH_2 groups, a typical feature of such molecules.⁷⁸ The resulting “extra” node, from a predominantly antibonding interaction with CH_2 π -type orbitals, is apparent.

In the disubstituted case, the MOs form quasi-degenerate pairs, each pair consisting of helices of opposite handedness. The splitting within each pair of helical MOs is 2 meV or less for the specific case of methyl. Larger splittings may be achieved by chemical design, especially with substituents that are single-faced π donors and acceptors, which we will explore in future work. By

visual inspection of the “internal” part of the helical π system shown in Figure 1, from end-to-end the HOMO-3 and HOMO-2 approximately twist by $\pm 90^\circ$. By inspection of Figure 7, the HOMO-1 and HOMO approximately twist $\pm 270^\circ$; the LUMO and LUMO+1 twist $\pm 450^\circ$. For every energy level, there is an extra $\pm 180^\circ$ twist in the MOs. The correspondence with the Hückel MOs is clear. The actual uneven distribution of the helical twist along the cumulene, alluded to above and occurring even at the Hückel level, may have consequences for prospective magnetic properties of the even $[n]$ cumulenes.^{6,79}

What does it mean that a molecular orbital is helical? The description is intuitive, but perhaps it is worth saying that (a) it is the nodal surface that is propagating helically in each orbital; (b) any choice of isovalue will also propagate helically in space; (c) it is the number of nodal surfaces along the carbon axis that increases for every quasi-degenerate energy level with rising energy.

■ CYCLIC VERSUS COARCTATE MÖBIUS SYSTEMS

In the following sections we return to the simple Hückel model to explore the relation between Heilbronner's Möbius systems and even $[n]$ cumulenes; the latter are by orbital topology coarctate Möbius systems.

There is an inevitable confusion at work between Hückel and Möbius *models*, *topologies*, and *aromaticities*—we will try hard to keep things straight. All the *models* we use are Hückel-type models, meaning by that only that there enters into conjugation one carbon 2p orbital per atom (or in the description of Herges coarctate systems two orthogonal 2p orbitals per atom). The set of orbital interactions (or the Hamiltonian) for any model may be referred to as Hückel or Möbius type “*system*”—the reference here is to whether the cyclic closure of the ring is accomplished with one or the other topology, signaled by the + or – factor of the $1, n$ off-diagonal matrix elements. We will also use the term Hückel or Möbius “*basis*”, or “*topology*”, in an equivalent way to “*system*.” Aromaticity, Hückel or Möbius, with all its tradition, measures, and complexities, not to speak of its contemporary hype-strewn exercise, will refer simplistically to whether the $4n+2$ or $4n$ rule for closed shell character is observed.

■ MÖBIUS CYCLOBUTADIENE AND ALLENE

We begin with a four-site model (4), which corresponds to a Möbius orbital interaction system for cyclobutadiene (unachievable in a real system, easy here in a theoretical model) and, equivalently, the coarctate basis of allene. For both Möbius cyclobutadiene and allene, the twist in the basis orbitals is continuous, 45° for each neighboring orbital (Figure 8a). Thus, enters the attenuation factor $k = \cos(45^\circ)$.

$$H = \begin{bmatrix} \alpha & k\cdot\beta & 0 & -k\cdot\beta \\ k\cdot\beta & \alpha & k\cdot\beta & 0 \\ 0 & k\cdot\beta & \alpha & k\cdot\beta \\ -k\cdot\beta & 0 & k\cdot\beta & \alpha \end{bmatrix} \quad (4)$$

To see the special features of this Hückel model (4) for Möbius cyclobutadiene, or coarctate allene, we show the corresponding Hückel Hamiltonian matrix for simple (square) cyclobutadiene (5).

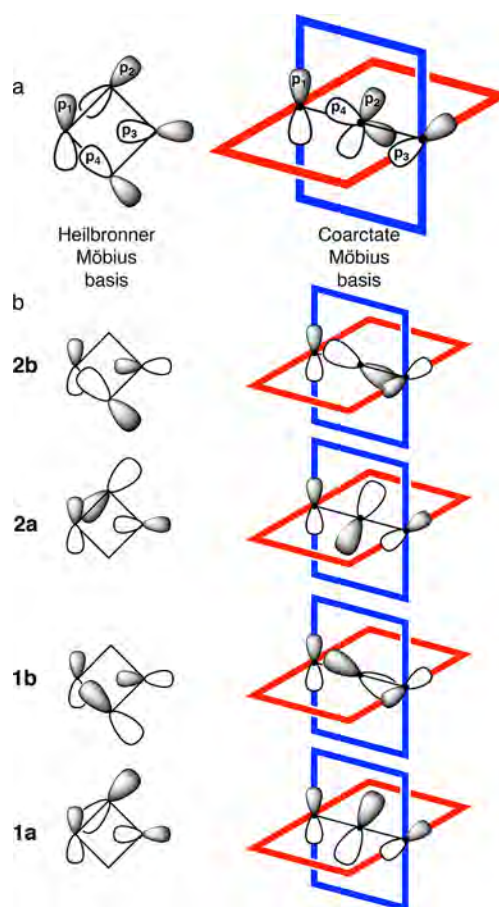


Figure 8. Basis set (a) and MOs (b) for a four-site Hückel model (eq 4). The result can be depicted in two different ways, depending on the molecular geometry in which the model is applied. The Heilbronner Möbius basis of cyclobutadiene (left) and the coarctate Möbius basis of allene (right) have the same orbital topology, but the three-dimensional depictions have the morphology of a cyclic and a coarctate Möbius strip, respectively. Note the cyclic Möbius system is drawn without perspective and should be considered as a diagrammatic depiction.

Table 2. Hückel Model MOs for Cyclobutadiene and Allene Calculated from the Möbius Basis Shown in Figure 8

		LCAO		
		Atom 1	Atom 2	Atom 3
		p_1	p_2	p_3
$\epsilon \cdot \beta^{-1}$	MO		p_4	
-1.00	2b	+ 0.50	+ 0.00 + 0.71	- 0.50
-1.00	2a	+ 0.50	- 0.71 + 0.00	+ 0.50
1.00	1b	+ 0.50	+ 0.00 - 0.71	- 0.50
1.00	1a	+ 0.50	+ 0.71 + 0.00	+ 0.50

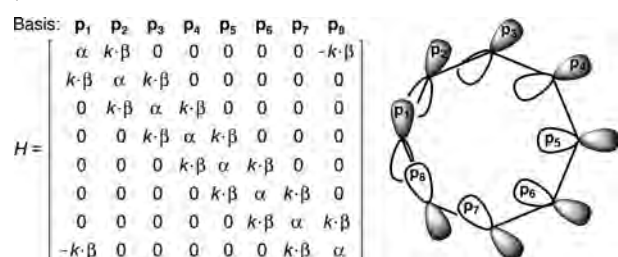
$$H = \begin{bmatrix} \alpha & \beta & 0 & \beta \\ \beta & \alpha & \beta & 0 \\ 0 & \beta & \alpha & \beta \\ \beta & 0 & \beta & \alpha \end{bmatrix} \quad (5)$$

Two differences are apparent; the Möbius/coarctate system introduces a reduction or scaling factor k on the near neighbor interactions, with $k < 1$. This is just the realism of the near neighbor resonance integral—it must be reduced from β as the system starts and continues twisting. All k are assumed equal in the most simplistic model of a cyclic Möbius polyene; as we mentioned, they need not be equal in a real molecule, and we will return to this point.

Much more significant is the real distinction between Hückel and Möbius topologies, even as it seems to hide in just one entry—the sign (+ for Hückel, – for Möbius) of the 1,4 interaction. It makes a world of difference in the eigenvalue spectrum. This was Edgar Heilbronner's essential insight.⁴⁶

The Hückel model treatments of the two Möbius systems, cyclic and coarctate, are exactly the same; the resulting MOs are

Scheme 4. Hückel Matrix and Basis Set for Möbius Cyclooctatetraene



shown in Figure 8 and listed in Table 2. However, the “three-dimensional” depictions of the MOs give the two visually different results: those of a Möbius annulene (Figure 8, left) and the helical orbitals of allene (Figure 8, right).

The reader who knows well the orbitals of a cyclobutadiene or an allyl system may nevertheless find the eigenvectors of the Möbius topology Hamiltonian unfamiliar. They bear some introspection. Note first of all that each of the MOs (Möbius cyclobutadiene or allene) is localized on only 3 of the 4 basis orbitals (p_1, p_2 , and p_3 ; or p_1, p_4 , and p_3), and each has an “allylic” form with terminal coefficients smaller than the middle one. Second, the two components of each degenerate orbital are identical in their makeup, but of opposite helicity. For Möbius cyclobutadiene, this shows up in different atoms (2 or 4) carrying

a large orbital contribution; for the coarctate allene, the two orbitals are on the same center.

The three-dimensional depictions of the MOs in Figure 8 show clearly the close connection between the cyclic Möbius systems Heilbronner originally described and the cumulenic systems. Starting out with Möbius cyclobutadiene, the set of helical MOs of allene is the result of fusing basis orbitals p_2 and p_4 onto the same atom. Considering the orbital topology and C_2 symmetry, 1,3-disubstituted allene certainly merits to be recognized as a coarctate Möbius system.

A final point on the energy levels of a Möbius cyclobutadiene or an allene: the energies of their orbitals are identical at the Hückel level. This identity will not persist for Möbius cyclooctatetraene and pentatetraene, for reasons we will explain in the next section. And while we will return to a comparison of the energetics of Möbius cyclopolyenes and coarctate even [n]cumulenes, the equal π -electron energies of allene and Möbius cyclobutadiene make it clear that there is no particular stabilization accruing to either, even if they are both closed shell molecules.

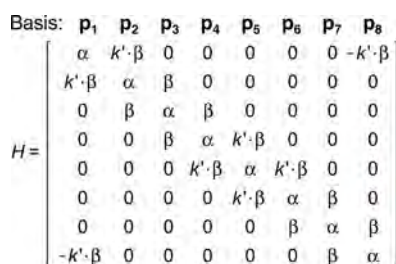
■ MÖBIUS CYCLOOCTATETRAENE AND [4]CUMULENE: A DIFFERENCE

We proceed with the Hückel treatment for Möbius cyclooctatetraene and [4]cumulene. Möbius cyclooctatetraene was also treated at the Hückel level of theory by Mckee et al.⁵⁴ The assumed Möbius conformation of cyclooctatetraene is an idealized structure with the total 180° twist evenly distributed through the basis (see Scheme 4, right). In the eight-site model Hamiltonian (Scheme 4, left) all nearest neighbor interactions are attenuated by $k = \cos(22.5^\circ)$. And the characteristic Möbius joining, via $-k\beta$, is there.

The coarctate Möbius basis of [4]cumulene differs in a subtle but significant way from that of Möbius cyclooctatetraene. While the total twist in the basis of the two is the same (180°), the twist cannot be evenly distributed in [4]cumulene. Rather than eight twists of 22.5° , there are four twists of 45° , and four of 0° (p_2-p_3 , p_3-p_4 , p_6-p_7 , and p_7-p_8), as one may see in Scheme 5. The characteristic Möbius juncture ($-k'\beta$) is there, but the off-diagonal resonance integral values differ from the cyclic system, as some nearest neighbor interactions are attenuated by $k' = \cos(45^\circ)$ and others are not attenuated.

While the orbitals of the cyclic Möbius system and the cumulene are similar (see Figure 9), their energies now differ, albeit slightly. As Scheme 6 (and Tables S1 and S2) shows, the [4]cumulene eigenvalues are slightly higher in energy (β is negative) than those of Möbius cyclooctatetraene. For the 4-orbital systems discussed in the previous section, the eigenvalues of the Möbius annulene and coarctate analogue Hückel matrices

Scheme 5. Hückel Matrix and Basis Set for Pentatetraene



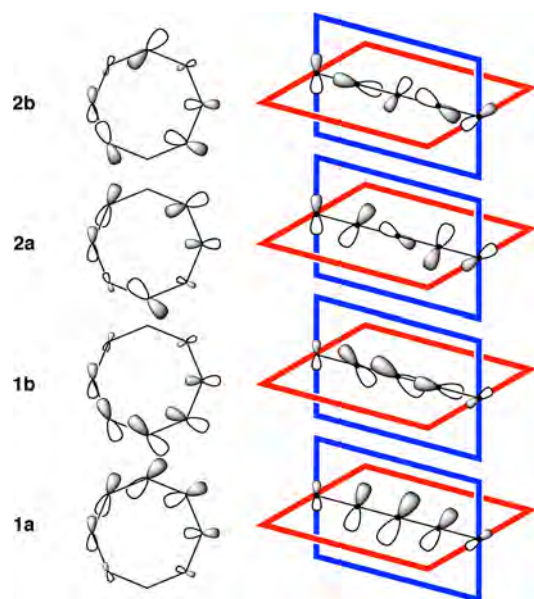
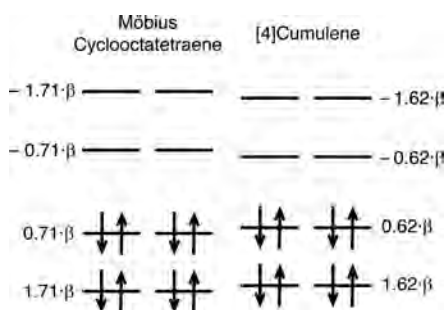


Figure 9. Bonding MOs of cyclic Möbius cyclooctatetraene (left) and coarctate Möbius [4]cumulene (right). Note the cyclic Möbius system is drawn without perspective and should be considered as a diagrammatic depiction.

Scheme 6. Energy Levels of Möbius Cyclooctatetraene (Scheme 4) and [4]Cumulene (Scheme 5) Compared



are identical; they are not for 8-orbital systems or higher n . More generally, in some coarctate and simple cyclic systems, the distribution of twist along the basis (expressed by the values of k , the attenuation factor) leads to no difference in the energy levels (for instance allene). But in some other cases, differences emerge. This is an interesting finding; the beginnings of a discussion may be found in the [Supporting Information](#). The reader will have noted another example, starting from the rectilinear basis (Scheme 2) and the coarctate Möbius basis (Scheme 5) of [4]cumulene yields the same energy levels, cf. Figure 4 and 9, Tables 1 and S2. The difference between the two starting points is a basis set rotation.

Real Möbius Systems. The estimate of the overlap attenuation factor k is nontrivial for real cyclic Möbius molecules and was explored in some detail in the work of Mckee et al.⁵⁴ It is clear from their results that the attenuated overlap in Möbius annulenes implies for small rings that only an overall relatively weak resonance stabilization can be achieved. This is a consequence of unavoidable coupling to the underlying σ system.

As much as we admire the molecular architecture of Möbius systems, we urge the community to pay detailed attention to the overlap or its attenuation at every carbon along the ring; a concern others have alluded to as well.^{47,50,51,75} For larger rings

the overlap attenuation may not be so dramatic, in part because the ring can alleviate the attenuation through “writhe” in three dimensions.^{52,80,81} But one has to proceed carefully. If the overlap between two p-orbitals approaches 90° , the cyclic conjugation effectively breaks.^{56,57} Furthermore, the distribution of the twist changes the MO energetics and distribution, as we have shown. Literature reporting of dihedral angles, one way to gauge p-orbital overlap in Möbius systems, varies from reporting all dihedral angles,⁵⁷ through giving only the maximum dihedral angle,⁸² to reporting none;⁸³ the first option is strongly recommended. In the [Supporting Information](#), we describe an alternative algorithm for estimating overlap change along a ring.

■ ARE CUMULENES AROMATIC?

There are so many faces to aromaticity, a core concept of organic chemistry. It began with a notion of stability (part kinetic, part thermodynamic, the way chemistry is). Essential to the significance of benzenoid aromaticity is that benzene or phenyl groups could react, and yet their skeleton was preserved. In time other measures of aromaticity took hold—bond length equalization, ring currents, and NMR shielding constants.⁸⁴

The persistent feeling was that aromaticity was a good thing. The result, given the nature of human beings, was that more and more molecules were termed aromatic. The concept became enveloped in hype.⁸⁵

If the reader would like us to say that cumulenes, even or odd n ones, are aromatic or not, we will not go there. Instead we find it more productive to point out that there are some interesting similarities, and differences, between archetypical aromatic (or nonaromatic) molecules and cumulenes, Möbius or Hückel. We mention here that both Heilbronner and Zimmerman, pioneers in the field, had reservations about referring to Möbius systems as aromatic.^{46,51,63} Let us discuss these, class by class.

Hückel Annulenes. There is a vast literature on these. Succinctly, these follow in general Hückel’s rules, the $4n+2$ systems being closed shell molecules. The $4n+2$ cyclopolynes try to remain planar (not easy for $n = 2$). The double bonds in them localize for $n = 4$ and larger, yet ring currents persist.^{84,86} They are deservedly dubbed aromatic. The $4n$ systems have two electrons in a nonbonding degenerate orbital in a high-symmetry ring and are stabilized by bond-localization or out-of-plane distortion, as in the cyclooctatetraene archetype.

Möbius Cyclopolynes. Hückel’s rules are reversed, as Heilbronner taught us.⁴⁶ But aromaticity (identified initially as the closed-shell character of $4n$ cycles) is not attainable for small rings. The reason is the destabilizing combination of overlap attenuation as the molecules struggle to attain the Möbius topology, and the related strain in the σ -system of such rings.^{58,75} There are hints of achieving Möbius interactions in a 9-membered ring,^{87,88} and while kinetically persistent Möbius systems have been suggested for a 13-membered ring⁸⁹ they have not been reported to date for less than a [16]annulene⁵⁵ and [20] π porphyrin system.⁸³

Even [n]Cumulenes. As others before have pointed out,^{62,63} and as we rehearse in this paper, even [n]cumulenes furnish us with a Möbius π -system that is closed shell, and could be called aromatic. Whether the geometry is D_{2d} (unsubstituted), or lower (C_2 or C_1 if substituted), will influence the HOMO and LUMO e sets. But in either case, one has a situation close to that—near-degenerate highest filled and lowest unfilled orbital sets. And a gap between them. As we noted above, the π -electron stabilization in [4]cumulenes is less than in an 8-electron cyclic Möbius system. The latter has in addition its own problems in

strain in its σ system and is not a realistic conformation of cyclooctatetraene.⁷⁵

The difficulties in the synthesis of higher even $[n]$ cumulenes make it clear that a closed shell π -system is no guarantee of kinetic persistence; even the shortest cumulenes are quite reactive. We suspect that for even $[n]$ cumulenes a barrier to persistence is that the usual strategies of steric encumbrment do not work—it is hard for big substituents at the termini to effectively shield the center of the polyene rod. Perhaps protective rotaxane rings will do better.³⁹

We are just hesitant to call the closed-shell Möbius even $[n]$ cumulenes aromatic.

Odd $[n]$ Cumulenes. Until now we have focused solely on even $[n]$ cumulenes. However, as Zimmerman noted, odd $[n]$ cumulenes can be considered in terms of orbital topology as Hückel-type benzenoid systems with $4n+2$ electrons.⁹⁰ In Figure 10, the analogy between the archetype cyclic 6 electron

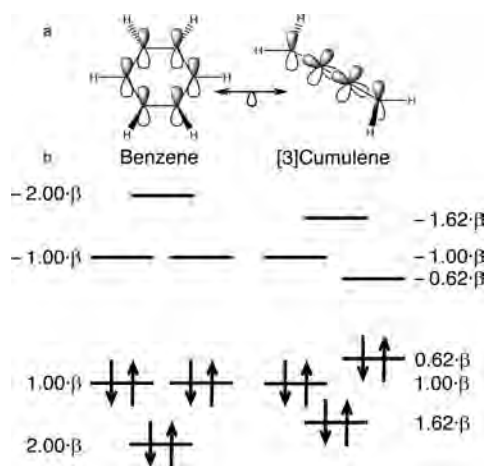


Figure 10. (a) Hückel aromatic orbital topology and (b) MO scheme of cyclic benzene, and coarctate [3]cumulene (butatriene).

aromatic system, benzene, and planar [3]cumulene (butatriene) is shown. There is no change of sign along the orbital basis, but the eigenvalue spectrum of [3]cumulene is different from benzene. Due to the reduced overlaps in the coarctate basis (Figure 10, right), there is no extra stabilization of the bonding MOs achieved by benzene, again a hint at the missing stability of cumulenes.

The clearest link between the cyclic and coarctate orbital topologies is displayed in their closed-shell geometries. The perpendicular geometry of allene is a 4-electron Möbius topology closed-shell system, and the planar [3]cumulene is a 6-electron Hückel topology closed-shell system. It is interesting to move from these points of similarity, to another one, now for the disfavored planar allene and “perpendicular” (D_{2d}) butatriene. Their energy levels are shown in Figure 11; clearly both are systems with a doubly occupied degenerate level. We will resist the temptation to call them antiaromatic; the switch from the closed shell systems of the favored conformations is clear.

These hypothetical conformations are in fact transition states for axial torsion of the molecules. As in the equivalent cyclic π -systems, they are likely to be diradicals, or subject to a Jahn–Teller distortion. We see again that the electronic structure of the cumulenes is governed by the same rules that govern the closed-shell structures of annulenes.

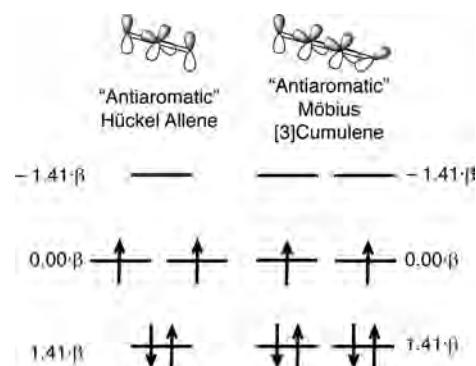


Figure 11. Orbital topology (top) and MO scheme (bottom) of Hückel “antiaromatic” planar allene (left) and Möbius “antiaromatic” perpendicular [3]cumulene.

THE EFFECT OF AXIAL TORSION

There is an alternative, intuitive way of reducing the symmetry in cumulenes. By applying torsion to the terminal trigonal carbon atoms, the symmetry of the (even and odd) unsubstituted $[n]$ cumulenes is reduced to D_{2v} .² Starting out in D_{2d} all three C_2 axes are retained in D_2 symmetry as the molecule is rotated toward the planar structure. In such an internal rotation all mirror symmetry is broken and the molecule becomes chiral. The same has to be true for an odd $[n]$ cumulene starting out in planar D_{2h} symmetry in an internal rotation toward the perpendicular (D_{2d}) structure, traversing a D_2 molecule. The orbitals grow helical. We see this clearly in Figure 12.

Starting from the D_{2d} optimized structure of [4]cumulene (dihedral angle 90°), for which, as we discussed, the orbitals can be rectilinear or helical. The orbitals remain helical as the axial dihedral angle evolves to 75° . Starting now from the optimized D_{2h} planar [3]cumulene, where there is no option for the orbitals to be helical, the MOs visually “obtain some helicity” already at a dihedral angle of 15° . Rotating the [3]cumulene further to 75° (an energetically disfavored conformation) the MOs appear just as helical as, and almost identical to, those of [4]cumulene at the same dihedral angle. Helical MOs also appear in terminally functionalized polyynes from axial torsion of the terminal groups when the molecules achieve the appropriate symmetry.^{8,91} Subjecting cumulenes to axial torsion is an interesting way to tune the electrohelicity effect in situ, which was also explored in separate studies by Imamura and Aoki,⁶ and Yakobson and co-workers.⁷

We note that even for ethylene, the simplest [1]cumulene, when one twists around the double bond into a D_2 geometry, eventually reaching a D_{2d} perpendicular one (highly unstable for the ground singlet state, but in fact the equilibrium geometry for the lowest triplet state of ethylene), that one clearly sees helicity in the orbitals.

TWO KINDS OF COARCTATE SYSTEMS AND HELICOGENICITY

Both even and odd $[n]$ cumulenes are coarctate, in the simple sense of two p systems mutually fused over the same atoms, or some subset of them. Yet we have seen that [4]cumulene and [3]cumulene, just to take a concrete example, are very different.

For [4]cumulene, helical and rectilinear (perpendicular) orbital sets are options, and α,ω -disubstitution immediately reveals the unique helical sets. For [3]cumulene, no simple substitution turns on electrohelicity, while a substantial axial twist does (along with destabilization).

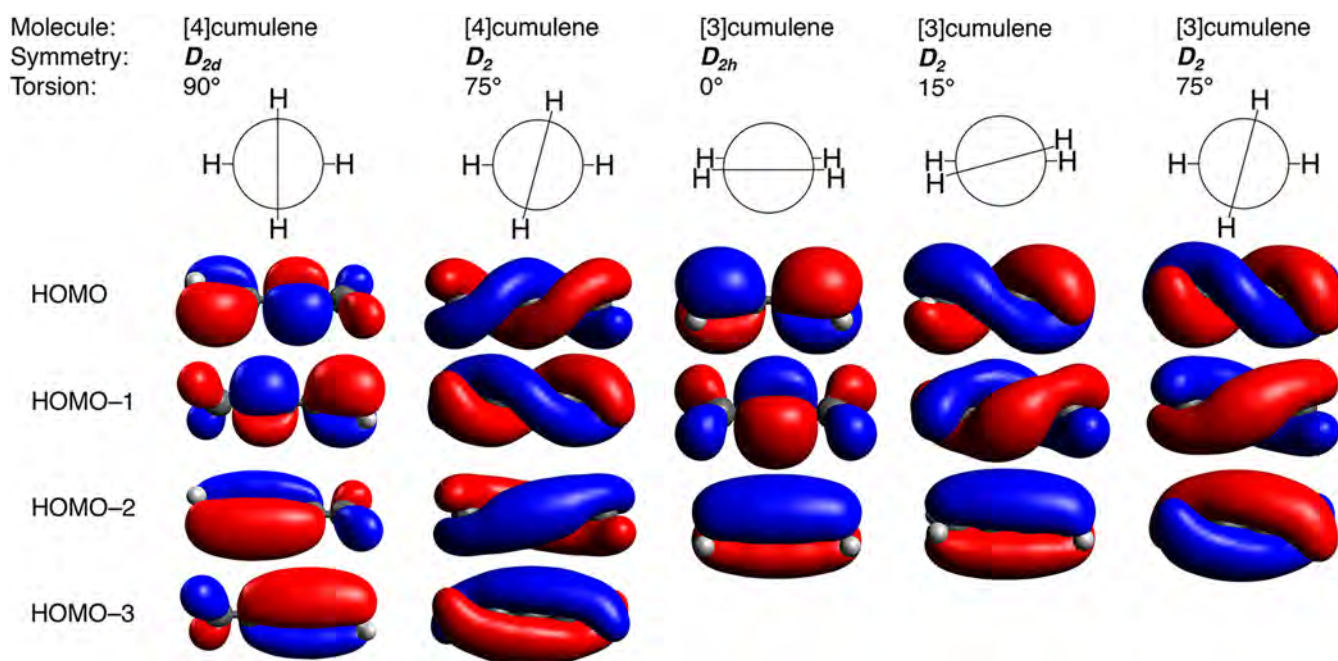


Figure 12. Reduction of symmetry to D_2 by axial torsion, i.e., manipulation of the H–C–C–H dihedral angle, resulting in helical orbitals. Bonding π orbitals are plotted. Left: [4]Cumulene in the optimized perpendicular structure of D_{2d} symmetry and the structure deformed to 75° torsion. Right: [3]cumulene in the optimized planar structure of D_{2h} symmetry and the structure constructed with 15° and 75° torsion.

We have already described the features of these two classes of systems. Let us point out the distinct difference between symmetries of [4]cumulene, [3]cumulene, and either of the two subjected to axial torsion. Shown in Figure 13 are the C_2

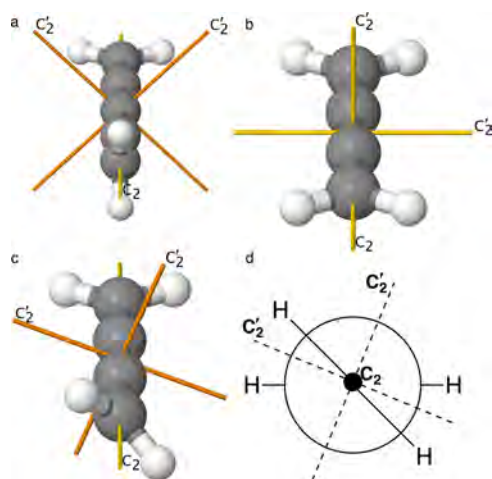


Figure 13. Helicogenic (orange) and non-helicogenic (yellow) C_2 symmetry axes. (a) D_{2d} [4]cumulene, two helicogenic axes, one non-helicogenic axis. (b) D_{2h} [3]cumulene, all three axes are nonhelicogenic and lie within mirror planes. (c) D_2 [3]cumulene constructed to a H–C–C–H dihedral angle of 45°, two helicogenic axes, one non-helicogenic axis. (d) Newman projection of the D_2 [3]cumulene.

symmetry axes of the three cases. In D_{2d} two of the axes are “helicogenic”; symmetry adaptation to one (or both) of these axes will yield helical orbitals. None of the rotation axes in D_{2h} are helicogenic. Yet subjecting the D_{2h} molecule to a (resisted) twist of the two CH_2 groups relative to each other—a deformation to D_2 symmetry—the mirror plane symmetry is removed, and two of the C_2 axes do become helicogenic, just like they are in D_{2d} geometry.

Specific symmetries allow otherwise orthogonal π systems to mix and become helical. The formation of helical symmetry-adapted MOs requires chirality, not surprising considering a helix is a chiral object. A general statement obtains for both even and odd $[n]$ cumulenes: *Nonplanar $[n]$ cumulenes without mirror-plane symmetry that have a helicogenic C_2 operation, one which rotates the (otherwise) perpendicular p_y and p_x orbital sets into each other, will have explicitly helical symmetry-adapted MOs.*

Let us mention a few examples of systems that do not fulfill the above statement. Unsubstituted [4]cumulene fails due to its mirror-plane symmetry. [3]Cumulene has mirror-plane symmetry and lacks helicogenic axes. Even 1,1-disubstituted- $[n]$ -cumulenes are achiral with C_{2v} symmetry. Yet even if the mirror-plane symmetry is broken by the substituents, the remaining C_2 axis is still nonhelicogenic (cf. Figure 13a). Two examples, 1,1-dimethyl-[4]cumulene (C_{2v}) and 1,1-diamino-[4]cumulene (C_2), are included in Supporting Information. Even n (α,ω)-disubstituted- $[n]$ cumulenes are, to our knowledge, the only type of cumulene system where the ground-state structures meet the symmetry requirements for helical orbitals.

Finally, we note that Herges has suggested that symmetry plays a similar important role for coarctate transition states.⁶⁹ Coarctate transition states are also isolobal to cumulenes. A clearer formulation of the connection between coarctate molecules, such as cumulenes, and coarctate transition states is left for future work.

CONCLUSIONS

We have presented a systematic derivation of the helical frontier orbitals of even-numbered $[n]$ cumulenes, including allene. Helicity, an option in describing the orbitals of the unsubstituted D_{2d} geometry, becomes a necessity for α,ω -disubstituted even $[n]$ cumulenes. The MOs are helical at the Hückel level of theory (or higher)—a procedure that requires no provisional knowledge of the helical depictions. The helical MOs are best considered as the result of describing the molecules as coarctate

Möbius systems, wherein two otherwise orthogonal sets of p-orbitals can mix. In contrast to a hypothetical Möbius annulene, even $[n]$ cumulenes are Möbius $4n$ systems where the basis functions are not uniformly “rotated”. The distribution of twist in the orbitals has implications for the orbital energetics in both the coarctate and the “normal” class of cyclic Möbius systems.

We have described structural and electronic analogies and differences between coarctate molecules, and their cyclic Hückel and Möbius counterparts. Our explicit derivation of the electrohelicity effects at the Hückel level of theory reinforces and extends the important foundational results of Hendon et al.⁸

There are interesting perspectives for future research in the helical orbital systems in coarctate Möbius molecules. Though the molecular orbitals are not quantum mechanical observables themselves, many observable properties can be derived from orbital theory. We hope that our clarification of the electrohelicity effect or helicogenicity will motivate further studies in electronic and magnetic effects in this peculiar class of molecules. Cyclic aromatic systems exhibit ring currents in the presence of a magnetic field, and this has been studied extensively for Möbius aromatic molecules^{47,51,53,54,87,92,93} and transition states.^{94–98} What intriguing effects are waiting to be found in coarctate Möbius systems with helical orbitals?

■ ASSOCIATED CONTENT

📄 Supporting Information

The Supporting Information is available free of charge on the ACS Publications website at DOI: [10.1021/acscentsci.8b00086](https://doi.org/10.1021/acscentsci.8b00086).

Orbital coefficients of $[4]$ cumulene and Möbius cyclooctatetraene; distributing the twist in Möbius systems; unitary transformations of matrices; algorithm for reporting twist in Möbius molecules; 1,1-disubstituted $[4]$ cumulene (PDF)

■ AUTHOR INFORMATION

Corresponding Authors

*(M.H.G.) E-mail: marc@chem.ku.dk.

*(R.H.) E-mail: rh34@cornell.edu.

ORCID

Marc H. Garner: [0000-0002-7270-8353](https://orcid.org/0000-0002-7270-8353)

Roald Hoffmann: [0000-0001-5369-6046](https://orcid.org/0000-0001-5369-6046)

Gemma C. Solomon: [0000-0002-2018-1529](https://orcid.org/0000-0002-2018-1529)

Notes

The authors declare no competing financial interest.

■ ACKNOWLEDGMENTS

We are grateful to Rainer Herges for his comments on the manuscript. We acknowledge the extensive online symmetry gallery of Otterbein University at <http://symmetry.otterbein.edu>, which greatly inspired us. M.H.G. and G.C.S. received funding from the Danish Council for Independent Research Natural Sciences and the Carlsberg Foundation.

■ ABBREVIATIONS

DFT: density functional theory; MO: molecular orbital

■ REFERENCES

- Buenker, R. J. Theoretical Study of the Rotational Barriers of Allene, Ethylene, and Related Systems. *J. Chem. Phys.* **1968**, *48*, 1368–1379.
- Dickerson, H.; Ferber, S.; Richardson, F. S. Molecular Orbital Calculations on the Optical Rotatory Properties of Chiral Allene Systems. *Theor. Chim. Acta* **1976**, *42*, 333–344.
- Deretey, E.; Shapiro, M.; Brumer, P. Chiral Molecules with Achiral Excited States: A Computational Study of 1,3-Dimethylallene. *J. Phys. Chem. A* **2001**, *105*, 9509–9517.
- Gu, X.; Kaiser, R. I.; Mebel, A. M. Chemistry of Energetically Activated Cumulenes—from Allene (H_2CCCH_2) to Hexapentaene ($H_2CCCCCH_2$). *ChemPhysChem* **2008**, *9*, 350–369.
- Ravagnan, L.; Manini, N.; Cinquanta, E.; Onida, G.; Sangalli, D.; Motta, C.; Devetta, M.; Bordoni, A.; Piseri, P.; Milani, P. Effect of Axial Torsion on Sp Carbon Atomic Wires. *Phys. Rev. Lett.* **2009**, *102*, 245502.
- Imamura, A.; Aoki, Y. Helical Molecular Orbitals around Straight-Chain Polyyne Oligomers as Models for Molecular Devices. *Chem. Phys. Lett.* **2013**, *590*, 136–140.
- Liu, M.; Artyukhov, V. I.; Lee, H.; Xu, F.; Yakobson, B. I. Carbyne from First Principles: Chain of C Atoms, a Nanorod or a Nanorope. *ACS Nano* **2013**, *7*, 10075–10082.
- Hendon, C. H.; Tiana, D.; Murray, A. T.; Carbery, D. R.; Walsh, A. Helical Frontier Orbitals of Conjugated Linear Molecules. *Chem. Sci.* **2013**, *4*, 4278–4284.
- Yu, S.; Ma, S. How Easy Are the Syntheses of Allenes? *Chem. Commun.* **2011**, *47*, 5384–5418.
- Rivera-Fuentes, P.; Diederich, F. Allenes in Molecular Materials. *Angew. Chem., Int. Ed.* **2012**, *51*, 2818–2828.
- Kuehnel, M. F.; Schlöder, T.; Riedel, S.; Nieto-Ortega, B.; Ramirez, F. J.; López Navarrete, J. T.; Casado, J.; Lentz, D. Synthesis of the Smallest Axially Chiral Molecule by Asymmetric Carbon–Fluorine Bond Activation. *Angew. Chem., Int. Ed.* **2012**, *51*, 2218–2220.
- Lechel, T.; Pfrengle, F.; Reissig, H.-U.; Zimmer, R. Three Carbons for Complexity! Recent Developments of Palladium-Catalyzed Reactions of Allenes. *ChemCatChem* **2013**, *5*, 2100–2130.
- Hashimoto, T.; Sakata, K.; Tamakuni, F.; Dutton, M. J.; Maruoka, K. Phase-Transfer-Catalyzed Asymmetric Synthesis of Tetrasubstituted Allenes. *Nat. Chem.* **2013**, *5*, 240–244.
- Soriano, E.; Fernandez, I. Allenes and Computational Chemistry: From Bonding Situations to Reaction Mechanisms. *Chem. Soc. Rev.* **2014**, *43*, 3041–3105.
- Ye, J.; Ma, S. Conquering Three-Carbon Axial Chirality of Allenes. *Org. Chem. Front.* **2014**, *1*, 1210–1224.
- Tap, A.; Blond, A.; Wakchaure, V. N.; List, B. Chiral Allenes Via Alkynologous Mukaiyama Aldol Reaction. *Angew. Chem., Int. Ed.* **2016**, *55*, 8962–8965.
- Alonso, J. M.; Quiros, M. T.; Munoz, M. P. Chirality Transfer in Metal-Catalyzed Intermolecular Addition Reactions Involving Allenes. *Org. Chem. Front.* **2016**, *3*, 1186–1204.
- Chu, W.-D.; Zhang, L.; Zhang, Z.; Zhou, Q.; Mo, F.; Zhang, Y.; Wang, J. Enantioselective Synthesis of Trisubstituted Allenes Via Cu(I)-Catalyzed Coupling of Diazoalkanes with Terminal Alkynes. *J. Am. Chem. Soc.* **2016**, *138*, 14558–14561.
- Kuhn, R.; Fischer, H.; Fischer, H. Über Kumulene, XVII. Darstellung von Pentatetraenen. *Chem. Ber.* **1964**, *97*, 1760–1766.
- Skattebøl, L. A Novel Route to Cumulenes. The Addition of Dihalocarbenes to 2,5-Dimethyl-2,3,4-Hexatriene. *Tetrahedron Lett.* **1965**, *6*, 2175–2179.
- Jochims, J. C.; Karich, G. 1,5-Di-tert.-Butyl-1,5-Diphenyl-Pentatetraen. *Tetrahedron Lett.* **1974**, *15*, 4215–4218.
- Jochims, J. C.; Karich, G. The Ground State Geometry of a Pentatetraene. *Tetrahedron Lett.* **1976**, *17*, 1395–1398.
- Ripoll, J. L. Synthesis of Pentatetraene by Thermal Decomposition of a Vinylallene. *J. Chem. Soc., Chem. Commun.* **1976**, 235–236.
- Oostveen, E. A.; Elsevier, C. J.; Meijer, J.; Vermeer, P. Tert-Butylsilver-Induced 1,5-Substitution in Some 2,4-Pentadiynyl Methanesulfonates. A Novel Route to Di- and Trisubstituted Pentatetraenes. *J. Org. Chem.* **1982**, *47*, 371–373.
- Irgangtinger, H.; Götzmann, W. Structure Determinations of Pentatetraenes—Comparison of the Structures of Cumulenes. *Angew. Chem., Int. Ed. Engl.* **1986**, *25*, 340–342.

- (26) Nader, F. W.; Brecht, A. Wittig Reaction with Carbon Suboxide: Synthesis of Dimethyl 1,5-Diphenyl-1,2,3,4-Pentatetraenedicarboxylate. *Angew. Chem., Int. Ed. Engl.* **1986**, *25*, 93–94.
- (27) Nader, F. W.; Brecht, A.; Kreisz, S. Chemie der Kumulene, 7. Synthese von 1,2,3,4-Pentatetraen-1,5-Dicarbonsäure-Derivaten durch Wittig-Reaktion mit 1-H-Allen-1,3-Dicarbonsäuremonoesterchloriden. *Chem. Ber.* **1986**, *119*, 1208–1216.
- (28) Tokitoh, N.; Suzuki, T.; Ando, W. A Facile Synthesis and Novel Reactions of 1, 2, 3, 4-Pentatetraene Episulfides. *Tetrahedron Lett.* **1989**, *30*, 4271–4274.
- (29) Goulay, F.; Soorkia, S.; Meloni, G.; Osborn, D. L.; Taatjes, C. A.; Leone, S. R. Detection of Pentatetraene by Reaction of the Ethynyl Radical (C₂H) with Allene (CH₂=C=CH₂) at Room Temperature. *Phys. Chem. Chem. Phys.* **2011**, *13*, 20820–20827.
- (30) Roth, G.; Fischer, H. On the Way to Heptahexenyldiene Complexes: Trapping of an Intermediate with the Novel M=C=C=C=C=C=Cr₂ Moiety. *Organometallics* **1996**, *15*, 5766–5768.
- (31) Bildstein, B. Cationic and Neutral Cumulene Sp-Carbon Chains with Ferrocenyl Termini. *Coord. Chem. Rev.* **2000**, *206–207*, 369–394.
- (32) Bildstein, B.; Skibar, W.; Schweiger, M.; Kopacka, H.; Wurst, K. In situ synthesis of the first C₇ cumulene (Fc)₂C=C=C=C=C=C=C(Fc)₂ via deprotonation of its conjugate acid [(Fc)₂C₇H(Fc)₂]⁺BF₄[−] (Fc=ferrocenyl). *J. Organomet. Chem.* **2001**, *622*, 135–142.
- (33) Januszewski, J. A.; Wendinger, D.; Methfessel, C. D.; Hampel, F.; Tykwinski, R. R. Synthesis and Structure of Tetraarylcumulenes: Characterization of Bond-Length Alternation Versus Molecule Length. *Angew. Chem., Int. Ed.* **2013**, *52*, 1817–1821.
- (34) Januszewski, J. A.; Tykwinski, R. R. Synthesis and Properties of Long [n]Cumulenes (n ≥ 5). *Chem. Soc. Rev.* **2014**, *43*, 3184–3203.
- (35) Wendinger, D.; Tykwinski, R. R. Odd [n]Cumulenes (n = 3, 5, 7, 9): Synthesis, Characterization, and Reactivity. *Acc. Chem. Res.* **2017**, *50*, 1468–1479.
- (36) Szafert, S.; Gladysz, J. A. Carbon in One Dimension: Structural Analysis of the Higher Conjugated Polyynes. *Chem. Rev.* **2003**, *103*, 4175–4206.
- (37) Szafert, S.; Gladysz, J. A. Update 1 Of: Carbon in One Dimension: Structural Analysis of the Higher Conjugated Polyynes. *Chem. Rev.* **2006**, *106*, PR1–PR33.
- (38) Chalifoux, W. A.; Tykwinski, R. R. Synthesis of Polyynes to Model the sp-Carbon Allotrope Carbyne. *Nat. Chem.* **2010**, *2*, 967–971.
- (39) Franz, M.; Januszewski, J. A.; Wendinger, D.; Neiss, C.; Movsisyan, L. D.; Hampel, F.; Anderson, H. L.; Görling, A.; Tykwinski, R. R. Cumulene Rotaxanes: Stabilization and Study of [9]Cumulenes. *Angew. Chem., Int. Ed.* **2015**, *54*, 6645–6649.
- (40) Shi, L.; et al. Confined Linear Carbon Chains as a Route to Bulk Carbyne. *Nat. Mater.* **2016**, *15*, 634–639.
- (41) Walbrick, J. M.; Wilson, J. W.; Jones, W. M. A General Method for Synthesizing Optically Active 1,3-Disubstituted Allene Hydrocarbons. *J. Am. Chem. Soc.* **1968**, *90*, 2895–2901.
- (42) Waters, W. L.; Linn, W. S.; Caserio, M. C. Stereochemistry of Additions of Allenes. I. Methoxymercuration and Halogenation of 1,3-Dimethylallene. *J. Am. Chem. Soc.* **1968**, *90*, 6741–6749.
- (43) Waters, W. L.; Caserio, M. C. Resolution and Absolute Configuration of 1,3-Dimethylallene. *Tetrahedron Lett.* **1968**, *9*, 5233–5236.
- (44) Crabbe, P.; Velarde, E.; Anderson, H. W.; Clark, S. D.; Moore, W. R.; Drake, A. F.; Mason, S. F. Optical Activity and Absolute Configuration of Chiral Allenes. *J. Chem. Soc. D* **1971**, *0*, 1261–1264.
- (45) Tykwinski, R. R. Carbyne: The Molecular Approach. *Chem. Rev.* **2015**, *15*, 1060–1074.
- (46) Heilbronner, E. Hückel Molecular Orbitals of Möbius-Type Conformations of Annulenes. *Tetrahedron Lett.* **1964**, *5*, 1923–1928.
- (47) Herges, R. Topology in Chemistry: Designing Möbius Molecules. *Chem. Rev.* **2006**, *106*, 4820–4842.
- (48) Schaller, G. R.; Topić, F.; Rissanen, K.; Okamoto, Y.; Shen, J.; Herges, R. Design and Synthesis of the First Triply Twisted Möbius Annulene. *Nat. Chem.* **2014**, *6*, 608.
- (49) Mauksch, M. *Excursions into Chemical Topology - Topomerisations, Chiral Enantiomerisations and Möbius Aromaticity*, Thesis, University of Erlangen-Nuremberg, 1999.
- (50) Mauksch, M.; Tsogoeva, S. B. Neutral Möbius Aromatics: Derivatives of the Pyrrole Congener Aza[11]Annulene as Promising Synthetic Targets. *Eur. J. Org. Chem.* **2008**, *2008*, 5755–5763.
- (51) Rzepa, H. S. Möbius Aromaticity and Delocalization. *Chem. Rev.* **2005**, *105*, 3697–3715.
- (52) Rappaport, S. M.; Rzepa, H. S. Intrinsically Chiral Aromaticity. Rules Incorporating Linking Number, Twist, and Writhe for Higher-Twist Möbius Annulenes. *J. Am. Chem. Soc.* **2008**, *130*, 7613–7619.
- (53) Castro, C.; Isborn, C. M.; Karney, W. L.; Mauksch, M.; Schleyer, P. v. R. Aromaticity with a Twist: Möbius [4n]Annulenes. *Org. Lett.* **2002**, *4*, 3431–3434.
- (54) McKee, W. C.; Wu, J. I.; Rzepa, H. S.; Schleyer, P. v. R. A Hückel Theory Perspective on Möbius Aromaticity. *Org. Lett.* **2013**, *15*, 3432–3435.
- (55) Ajami, D.; Oeckler, O.; Simon, A.; Herges, R. Synthesis of a Möbius Aromatic Hydrocarbon. *Nature* **2003**, *426*, 819–821.
- (56) Castro, C.; Chen, Z.; Wannere, C. S.; Jiao, H.; Karney, W. L.; Mauksch, M.; Puchta, R.; Hommes, N. J. R. v. E.; Schleyer, P. v. R. Investigation of a Putative Möbius Aromatic Hydrocarbon. The Effect of Benzannulation on Möbius [4n]Annulene Aromaticity. *J. Am. Chem. Soc.* **2005**, *127*, 2425–2432.
- (57) Ajami, D.; Hess, K.; Köhler, F.; Näther, C.; Oeckler, O.; Simon, A.; Yamamoto, C.; Okamoto, Y.; Herges, R. Synthesis and Properties of the First Möbius Annulenes. *Chem. - Eur. J.* **2006**, *12*, 5434–5445.
- (58) Fowler, P. W.; Jennekens, L. W. Geometric Localisation in Möbius π Systems. *Chem. Phys. Lett.* **2006**, *427*, 221–224.
- (59) Yoon, Z. S.; Osuka, A.; Kim, D. Möbius Aromaticity and Antiaromaticity in Expanded Porphyrins. *Nat. Chem.* **2009**, *1*, 113–122.
- (60) Martin-Santamaria, S.; Lavan, B.; Rzepa, H. S. Möbius Aromatics Arising from a C=C=C Ring Component. *Chem. Commun.* **2000**, 1089–1090.
- (61) Martin-Santamaria, S.; Rzepa, H. S. Möbius and Huckel Molecular Orbitals Arising from C=C=C Components in Annulene Rings. *J. Chem. Soc., Perkin Trans.* **2000**, *2*, 2372–2377.
- (62) Fischer, H.; Kollmar, H. Zur Invarianz in der LCAO MO Theorie. *Theor. Chim. Acta* **1968**, *12*, 344–348.
- (63) Zimmerman, H. E. Möbius-Hückel Concept in Organic Chemistry. Application of Organic Molecules and Reactions. *Acc. Chem. Res.* **1971**, *4*, 272–280.
- (64) Herges, R. Organizing Principle of Complex Reactions and Theory of Coarctate Transition States. *Angew. Chem., Int. Ed. Engl.* **1994**, *33*, 255–276.
- (65) Herges, R. Coarctate Transition States: The Discovery of a Reaction Principle. *J. Chem. Inf. Model.* **1994**, *34*, 91–102.
- (66) Berger, C.; Bresler, C.; Dilger, U.; Geuenich, D.; Herges, R.; Röttele, H.; Schröder, G. A Spontaneous Fragmentation: From the Criegee Zwitterion to Coarctate Möbius Aromaticity. *Angew. Chem., Int. Ed.* **1998**, *37*, 1850–1853.
- (67) Birney, D. M. Electrocyclic Ring Openings of 2-Furylcarbene and Related Carbenes: A Comparison between Pseudopericyclic and Coarctate Reactions. *J. Am. Chem. Soc.* **2000**, *122*, 10917–10925.
- (68) Young, B. S.; Herges, R.; Haley, M. M. Coarctate Cyclization Reactions: A Primer. *Chem. Commun.* **2012**, *48*, 9441–9455.
- (69) Herges, R. Coarctate and Pseudocoarctate Reactions: Stereochemical Rules. *J. Org. Chem.* **2015**, *80*, 11869–11876.
- (70) Karadakov, P.; Enchev, V.; Fratev, F.; Castano, O. Electronic Structure of Möbius Annulenes. *Chem. Phys. Lett.* **1981**, *83*, 529–532.
- (71) Coulson, C. A.; Rushbrooke, G. S. Note on the Method of Molecular Orbitals. *Math. Proc. Cambridge Philos. Soc.* **1940**, *36*, 193–200.
- (72) Cotton, F. A. *Chemical Applications of Group Theory*, 3rd ed.; John Wiley & Sons, Inc.: New York, 1990.
- (73) Wilson, E. B.; Cross, P. C.; Decius, J. C. *Molecular Vibrations: The Theory of Infrared and Raman Vibrational Spectra*; McGraw-Hill: New York, 1955.

- (74) Martin-Santamaria, S.; Rzepa, H. S. Twist Localisation in Single, Double and Triple Twisted Möbius Cyclacenes. *J. Chem. Soc., Perkin Trans.* **2000**, *2*, 2378–2381.
- (75) Havenith, R. W. A.; van Lenthe, J. H.; Jenneskens, L. W. Möbius Aromaticity in Small $[n]$ *trans*-Annulenes? *Int. J. Quantum Chem.* **2001**, *85*, 52–60.
- (76) Zhao, Y.; Truhlar, D. G. The M06 Suite of Density Functionals for Main Group Thermochemistry, Thermochemical Kinetics, Non-covalent Interactions, Excited States, and Transition Elements: Two New Functionals and Systematic Testing of Four M06-Class Functionals and 12 Other Functionals. *Theor. Chem. Acc.* **2008**, *120*, 215–241.
- (77) Frisch, M. J., et al. *Gaussian 09*, Rev. D.01; Gaussian, Inc.: Wallingford, CT, 2013.
- (78) Wu, J. I. C.; Schleyer, P. v. R. Hyperconjugation in Hydrocarbons: Not Just a “Mild Sort of Conjugation”. *Pure Appl. Chem.* **2013**, *85*, 921.
- (79) Sarbadhikary, P.; Shil, S.; Panda, A.; Misra, A. A Perspective on Designing Chiral Organic Magnetic Molecules with Unusual Behavior in Magnetic Exchange Coupling. *J. Org. Chem.* **2016**, *81*, 5623–5630.
- (80) Schaller, G. R.; Herges, R. Möbius Molecules with Twists and Writhes. *Chem. Commun.* **2013**, *49*, 1254–1260.
- (81) Fowler, P. W.; Rzepa, H. S. Aromaticity Rules for Cycles with Arbitrary Numbers of Half-Twists. *Phys. Chem. Chem. Phys.* **2006**, *8*, 1775–1777.
- (82) Mohebbi, A. R.; Mucke, E.-K.; Schaller, G. R.; Köhler, F.; Sönnichsen, F. D.; Ernst, L.; Näther, C.; Herges, R. Singly and Doubly Twisted [36]Annulenes: Synthesis and Calculations. *Chem. - Eur. J.* **2010**, *16*, 7767–7772.
- (83) Anju, K. S.; Das, M.; Adinarayana, B.; Suresh, C. H.; Srinivasan, A. *meso*-Aryl [20] π Homoporphyrin: The Simplest Expanded Porphyrin with the Smallest Möbius Topology. *Angew. Chem., Int. Ed.* **2017**, *56*, 15667–15671.
- (84) Minkin, V. I.; Glukhovtsev, M. N.; Simkin, B. Y. *Aromaticity and Antiaromaticity: Electronic and Structural Aspects*; Wiley: New York, 1994.
- (85) Hoffmann, R. The Many Guises of Aromaticity. *Am. Sci.* **2015**, *103*, 18.
- (86) Mucke, E.-K.; Schönborn, B.; Köhler, F.; Herges, R. Stability and Aromaticity of Charged Möbius[4n]Annulenes. *J. Org. Chem.* **2011**, *76*, 35–41.
- (87) Mauksch, M.; Gogonea, V.; Jiao, H.; Schleyer, P. v. R. Monocyclic (CH)₉⁺—a Heilbronner Möbius Aromatic System Revealed. *Angew. Chem., Int. Ed.* **1998**, *37*, 2395–2397.
- (88) Bucher, G.; Grimme, S.; Huenerbein, R.; Auer, A. A.; Mucke, E.; Köhler, F.; Siegwarth, J.; Herges, R. Is the [9]Annulene Cation a Möbius Annulene? *Angew. Chem., Int. Ed.* **2009**, *48*, 9971–9974.
- (89) Mucke, E.-K.; Köhler, F.; Herges, R. The [13]Annulene Cation Is a Stable Möbius Annulene Cation. *Org. Lett.* **2010**, *12*, 1708–1711.
- (90) Zimmerman, H. E. 2. The Möbius-Hückel Treatment of Organic Systems and Reactions and MO Following as a Technique in Organic Chemistry. In *Organic Chemistry: A Series of Monographs*; Marchand, A. P.; Lehr, R. E., Eds.; Academic Press: New York, 1977; Vol. 35, pp 53–107.
- (91) Peeks, M. D.; Neuhaus, P.; Anderson, H. L. Experimental and Computational Evaluation of the Barrier to Torsional Rotation in a Butadiyne-Linked Porphyrin Dimer. *Phys. Chem. Chem. Phys.* **2016**, *18*, 5264–5274.
- (92) Pauling, L. The Diamagnetic Anisotropy of Aromatic Molecules. *J. Chem. Phys.* **1936**, *4*, 673–677.
- (93) Taubert, S.; Sundholm, D.; Pichierri, F. Magnetically Induced Currents in Bianthraquinodimethane-Stabilized Möbius and Hückel [16]Annulenes. *J. Org. Chem.* **2009**, *74*, 6495–6502.
- (94) Jiao, H.; von Ragué Schleyer, P. A Detailed Theoretical Analysis of the 1,7-Sigmatropic Hydrogen Shift: The Möbius Character of the Eight-Electron Transition Structure. *Angew. Chem., Int. Ed. Engl.* **1993**, *32*, 1763–1765.
- (95) Herges, R.; Jiao, H.; von Ragué Schleyer, P. Magnetic Properties of Aromatic Transition States: The Diels–Alder Reactions. *Angew. Chem., Int. Ed. Engl.* **1994**, *33*, 1376–1378.
- (96) Mauksch, M.; Tsogoeva, S. B. A Preferred Disrotatory 4n Electron Möbius Aromatic Transition State for a Thermal Electrocyclic Reaction. *Angew. Chem., Int. Ed.* **2009**, *48*, 2959–2963.
- (97) Schleyer, P. v. R.; Wu, J. I.; Cossio, F. P.; Fernandez, I. Aromaticity in Transition Structures. *Chem. Soc. Rev.* **2014**, *43*, 4909–4921.
- (98) Herges, R. Magnetic Properties of Aromatic Compounds and Aromatic Transition States. In *The Chemical Bond*; Wiley-VCH Verlag GmbH & Co. KGaA, Weinheim, 2014; pp 383–420.